

Глигор Јовановски

*Acta Cryst.* (1992), C48, 129–131

## Structure of 2,3-Diphenacylquinoxaline

By BRANKO KAITNER

*Laboratory of General and Inorganic Chemistry, Faculty of Science, University of Zagreb, PO Box 153, 41001 Zagreb, Croatia, Yugoslavia*

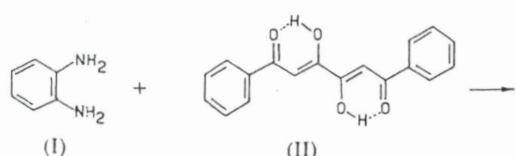
AND GLIGOR JOVANOVSKI AND IVANČO JANEV

*Institute of Chemistry, Faculty of Science, Cyril and Methodius University, 91000 Skopje, Macedonia, Yugoslavia*

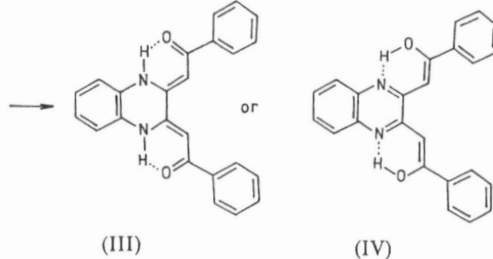
(Received 16 February 1991; accepted 21 June 1991)

**Abstract.**  $C_{24}H_{18}N_2O_2$ ,  $M_r = 366.42$ , orthorhombic,  $Pbcn$ ,  $a = 23.254$  (6),  $b = 11.495$  (3),  $c = 6.944$  (2) Å,  $V = 1856.2$  (9) Å<sup>3</sup>,  $Z = 4$ ,  $D_x = 1.31$  g cm<sup>-3</sup>,  $\lambda(Cu K\alpha) = 1.54178$  Å,  $\mu = 6.356$  cm<sup>-1</sup>,  $F(000) = 768$ ,  $T = 293$  K,  $R = 0.048$ ,  $wR = 0.056$  for 1042 unique reflections with  $I \geq 2\sigma(I)$ . The structure is built up of discrete molecules held together by van der Waals interactions only. The molecule is placed in the special position 4(c) possessing crystallographic  $C_2$  symmetry. An intramolecular N—H···O hydrogen bond is present in the structure.

**Introduction.** The 3,4-dihydroxy-1,6-diphenyl-2,4-hexadiene-1,6-dione (II) is a product of the reaction between acetophenone and diethyl oxalate (Kaitner, Jovanovski & Janev, 1992). This substance reacts with *o*-phenylenediamine (I) and the resulting product is 2,3-diphenacylquinoxaline. It was not possible to distinguish between tautomers (III) and (IV) by infrared spectroscopy. An X-ray structure determination was therefore undertaken.



0108-2701/92/010129-03\$03.00



**Experimental.** The title compound was obtained upon mixing and refluxing ethanol solutions of *o*-phenylenediamine and 3,4-dihydroxy-1,6-diphenyl-2,4-hexadiene-1,6-dione in an equimolar ratio. The microcrystalline product was recrystallized from ethanol; red-orange needle-shaped crystals were used in the structure determination.

Accurate cell dimensions and the crystal orientation matrix were determined on a Philips PW1100 automatic four-circle diffractometer by a least-squares treatment of the setting angles of 16 reflections in the range  $7 < \theta < 15^\circ$ . Crystal dimensions were  $0.15 \times 0.16 \times 0.30$  mm. The intensities of reflections  $h$  0 to 29,  $k$  0 to 15,  $l$  0 to 9 with  $2 < \theta < 70^\circ$  were measured using the  $\theta$ – $2\theta$  scan mode; scan width  $1.0^\circ$ ; scan speed  $0.04^\circ$  s<sup>-1</sup>; graphite-monochromatized  $Cu K\alpha$  radiation. Intensities of

© 1992 International Union of Crystallography

Table 1. Final atomic coordinates ( $\times 10^4$ ,  $\times 10^3$  for HN) for refined atoms and equivalent isotropic thermal parameters ( $\text{\AA}^2 \times 10^4$ ) for non-hydrogen atoms

	$U_{\text{eq}} = \frac{1}{3} \sum_i \sum_j U_{ij} a_i^* a_j^* \mathbf{a}_i \cdot \mathbf{a}_j$ .	$x$	$y$	$z$	$U_{\text{eq}}$
O	1446 (1)	127 (2)	673 (2)	506 (6)	
N	550 (1)	1274 (2)	1870 (3)	416 (6)	
C1	286 (1)	4417 (2)	2195 (5)	662 (9)	
C2	572 (1)	3383 (2)	1906 (4)	542 (9)	
C3	286 (1)	2335 (2)	2186 (3)	429 (7)	
C4	302 (1)	228 (2)	2147 (3)	372 (6)	
C5	598 (1)	-780 (2)	1790 (3)	394 (7)	
C6	1179 (1)	-789 (2)	1086 (3)	399 (6)	
C7	1477 (1)	-1923 (2)	869 (3)	421 (8)	
C8	1934 (1)	-2013 (2)	-443 (4)	532 (9)	
C9	2240 (1)	-3038 (3)	-583 (5)	693 (12)	
C10	2112 (1)	-3975 (3)	575 (5)	682 (12)	
C11	1659 (1)	-3903 (2)	1870 (5)	649 (11)	
C12	1345 (1)	-2887 (2)	2000 (4)	527 (9)	
HN	89 (1)	124 (2)	120 (5)	—	

Table 2. Bond distances ( $\text{\AA}$ ) and bond angles ( $^\circ$ )

O—C6	1.256 (3)	C4—C5	1.370 (3)
N—C3	1.383 (3)	C5—C6	1.437 (3)
N—C4	1.347 (3)	C6—C7	1.484 (3)
N—HN	0.93 (3)	C7—C8	1.404 (3)
C1—C1 <sup>i</sup>	1.396 (3)	C7—C12	1.392 (3)
C1—C2	1.377 (3)	C8—C9	1.380 (4)
C2—C3	1.390 (3)	C9—C10	1.377 (5)
C3—C3 <sup>i</sup>	1.400 (3)	C10—C11	1.387 (4)
C4—C4 <sup>i</sup>	1.488 (3)	C11—C12	1.380 (3)
C3—N—C4	125.1 (2)	C5—C6—C7	118.7 (2)
C1 <sup>i</sup> —C1—C2	120.3 (2)	O—C6—C7	118.8 (2)
C1—C2—C3	119.8 (2)	C6—C7—C12	122.6 (2)
N—C3—C2	122.0 (2)	C6—C7—C8	119.0 (2)
C2—C3—C3 <sup>i</sup>	119.9 (2)	C8—C7—C12	118.3 (2)
N—C3—C3 <sup>i</sup>	118.1 (2)	C7—C8—C9	119.9 (2)
N—C4—C5	120.9 (2)	C8—C9—C10	121.0 (2)
N—C4—C4 <sup>i</sup>	116.8 (2)	C9—C10—C11	119.7 (3)
C4 <sup>i</sup> —C4—C5	122.3 (2)	C10—C11—C12	119.6 (3)
C4—C5—C6	122.7 (2)	C7—C12—C11	121.3 (2)
O—C6—C5	122.5 (2)		

Symmetry code: (i)  $-x, y, 0.5 - z$ .

three standard reflections measured throughout the data collection showed no evidence of crystal decay. A total of 1049 unique reflections were measured, and 1042 of them with  $F_o \geq 2\sigma(F_o)$  were used in structure solution and refinement. Data were corrected for Lorentz and polarization effects but not for absorption. The structure was solved by direct methods. Refinement was by full-matrix least squares (on  $F$ ) initially with isotropic and then with anisotropic thermal parameters for non-hydrogen atoms. At an intermediate stage of refinement, difference maps showed maxima in positions consistent with the locations of all the hydrogen atoms. The N-hydrogen atom was included in least-squares refinement. All other hydrogen atoms were placed in their geometrically expected positions (C—H 1.08  $\text{\AA}$ ) and included as riding atoms in structure-factor calculations but were not refined. An overall isotropic thermal parameter was allowed and refined for all

hydrogen atoms ( $U_{\text{iso}} = 0.078 \text{\AA}^2$ ). The final cycle of refinement included 132 variable parameters,  $R = 0.048$ ,  $wR = 0.056$ , goodness of fit = 0.81,  $w = 1/(\sigma^2 F_o + 0.00588 F_o^2)$ ; the maximum shift/e.s.d. was  $-0.016$  ( $x$  coordinate of HN). Largest peaks and valleys in final difference map were  $+0.21$  and  $-0.25 \text{ e \AA}^{-3}$ ; there were no chemically significant features. Scattering factors and anomalous-dispersion corrections were taken from *International Tables for X-ray Crystallography* (1974, Vol. IV, pp. 99–101, 149–150). All calculations were performed on a UNIVAC 1110 computer of the Zagreb University Computing Centre and on an IBM PC/AT compatible microcomputer (microprocessor 80386/25 MHz and mathematical coprocessor 80387) using *MULTAN80* (Main, Fiske, Hull, Lessinger, Germain, Declercq & Woolfson, 1980) and the *CRYSRULER* package (Rizzoli, Sangermano, Calestani & Andreetti, 1987). The *ORTEPII* program (Johnson, 1976) was used to generate the illustration.

**Discussion.** Final positional and equivalent isotropic thermal parameters are given in Table 1.\* Interatomic distances and bond angles are in Table 2. A view of the molecule perpendicular to the plane of the quinoxaline ring showing the atom-numbering

\* Lists of structure factors, anisotropic thermal parameters, H-atom coordinates, least-squares planes and selected torsion angles have been deposited with the British Library Document Supply Centre as Supplementary Publication No. SUP 54370 (15 pp.). Copies may be obtained through The Technical Editor, International Union of Crystallography, 5 Abbey Square, Chester CH1 2HU, England.

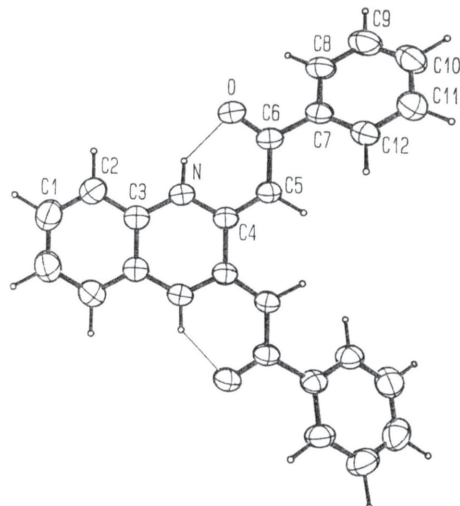


Fig. 1. A general view of the molecule showing the crystallographic numbering scheme. Thermal vibration ellipsoids scaled to 50% probability. Hydrogen atoms are shown as spheres of arbitrary radius. Hydrogen bonds (H···O) are indicated by thin lines.

scheme is given in Fig. 1. The molecules are not linked together by hydrogen bonds. The shortest intermolecular distance  $N \cdots C_6^i$  is 3.320 (3) Å [(i) =  $x$ ,  $-y$ ,  $z - 0.5$ ]. The molecule is in the special position 4(c) of the space group  $Pbcn$  possessing crystallographic symmetry  $C_2$ . The maximum deviation [0.071 (3) Å] of an atom from the least-squares plane through C1, C2, C3, N, C4, C5, C6, O is that of C2. The dihedral angle between this plane and the least-squares plane through the phenyl ring is 28.89 (5)°. The phenyl group geometries are normal.

There is an intramolecular  $N-H \cdots O$  hydrogen bond with carbonyl oxygen [ $O \cdots HN$  1.85 (3),  $N \cdots O$  2.602 (3) Å]. The  $C=O$  bond distance of 1.256 (3) Å corresponds to the expected value according to the molecular formula (III) (Stephen & Trotter, 1988; Corkern, Fronczeck, Gandour, Guo, Oliver & Watkins, 1988; Kaitner, Jovanovski & Janev, 1992). At the same time the  $N-C_4$  bond length of 1.347 (3) Å is very close to the value expected according to the formula (IV) (Wheatley, 1957; Morrow & Huddle, 1972). Some of the bond distances do not strictly belong to either formula (III) or (IV);  $C_4-C_5$  1.370 (3),  $C_5-C_6$  1.437 (3) and

$N-C_3$  1.383 (3) Å are midway between limiting values defining the above formulae.

This work was supported by the Federal (Belgrade) to BK and Republican (Zagreb, Croatia, and Skopje, Macedonia) Foundations for Scientific Research.

#### References

- CORKERN, J. A., FRONCZEK, F. R., GANDOUR, R. D., GUO, K., OLIVER, M. A. & WATKINS, S. F. (1988). *Acta Cryst. C44*, 1141–1143.
- JOHNSON, C. K. (1976). ORTEPII. Report ORNL-5138. Oak Ridge National Laboratory, Tennessee, USA.
- KAITNER, B., JOVANOVSKI, G. & JANEV, I. (1992). *Acta Cryst. C48*, 127–129.
- MAIN, P., FISKE, S. J., HULL, S. E., LESSINGER, L., GERMAIN, G., DECLERCQ, J.-P. & WOOLFSON, M. M. (1980). MULTAN80. A System of Computer Programs for the Automatic Solution of Crystal Structures from X-ray Diffraction Data. Univs. of York, England, and Louvain, Belgium.
- MORROW, J. C. & HUDDLE, B. P. (1972). *Acta Cryst. B28*, 1748–1753.
- RIZZOLI, C., SANGERMANO, V., CALESTANI, G. & ANDRETTI, G. D. (1987). *J. Appl. Cryst. 20*, 436–439.
- STEPHEN, E. V. & TROTTER, J. (1988). *Acta Cryst. C44*, 1459–1462.
- WHEATLEY, P. J. (1957). *Acta Cryst. 10*, 182–186.



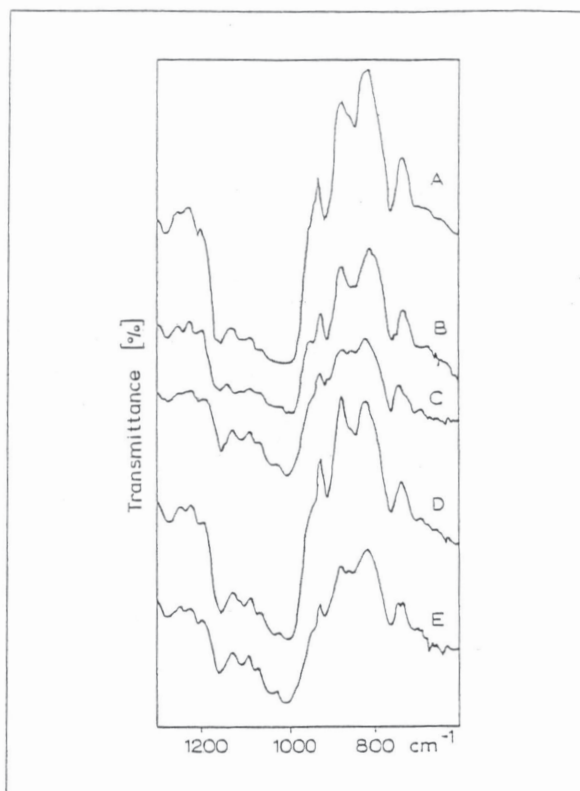


Fig. 1. Low frequency region of IR spectra of the amorphous dextran powder (A), the insoluble particle from the dextran solution (B), the induced dextran particulate matter (C), the dextran powder dried (D), and the dextran precipitate obtained from the amorphous dextran solution by water evaporation followed by drying (E)

Pharmazie 47 (1992), H. 9

Faculty of Technology<sup>1</sup>, University of Niš, Leskovac, and Institute of Chemistry<sup>2</sup>, Faculty of Science, Cyril and Methodius University, Skopje, Yugoslavia

#### Study on dextran particulation in bottled dextran solutions

M. D. CAKIĆ<sup>1</sup>, G. I. JOVANOVSKI<sup>2</sup>, V. B. VELJKOVIĆ<sup>1</sup>, M. L. LAZIĆ<sup>1</sup> and M. Z. STANKOVIĆ<sup>1</sup>

The insoluble particles in bottled dextran solutions sometimes formed during sterilization and long-term storage has drawn the attention of a number of investigators because of the great commercial and practical importance of the solution [1]. The insoluble particles are very closely related to the dextran used for the solution preparation [2]. Recently, it has been shown that the particulation occurs *via* a three-step mechanism: the isolation of a small amount of solution out of the main solution, the evaporation of water from the isolated droplets and the fall of dextran precipitate into the solution [3]. The water evaporation gives rise to the concentration of the isolated droplets, creating the favourable conditions for the phase transformation of dextran due to crystallization: the amorphous dextran from the solution becomes crystalline in the precipitate which is therefore insoluble [4].

In the present work the IR spectra and the X-ray powder diagrams of several dextran samples (amorphous dextran powder; dextran powder dried at 130 °C; and dextran precipitate obtained by water evaporation from the solution of the dextran and dried at 130 °C), the dextran particles isolated from commercial dextran solutions and the dextran particulate matter formed according to the mechanism described elsewhere [3] were studied. The main goal was to check the mechanism of formation and crystalline qualities of the insoluble particles.

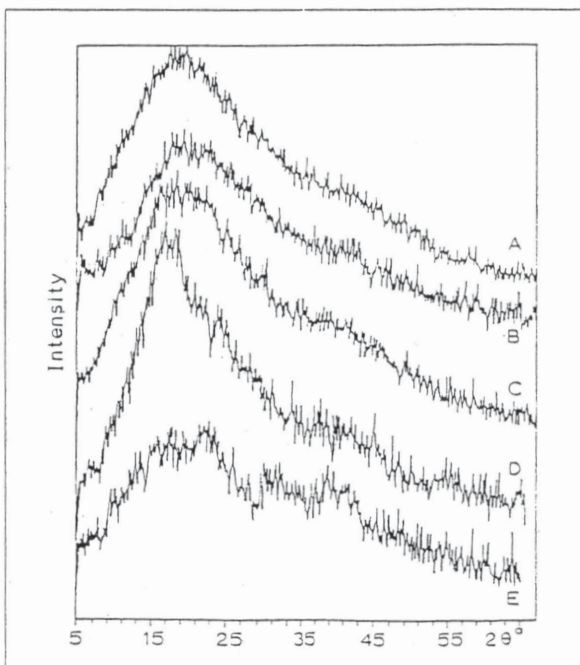


Fig. 2. X-ray powder diagrams. Key: see Fig. 1

The low-frequency region of the IR spectra of the amorphous dextran powder (A), the insoluble particle from the dextran solution (B), the induced dextran particulate matter (C), the dextran powder dried (D), and the dextran precipitate obtained from the amorphous dextran solution by water evaporation followed by drying (E) are shown in Fig. 1. Although the spectra are very similar to each other, an obvious difference can be seen at  $1047\text{ cm}^{-1}$ . Namely, the new clearly observed absorption band appears around  $1047\text{ cm}^{-1}$  in the spectra of the dextran samples B, C, D and E compared to that of the amorphous dextran (curve A in Fig. 1) in the same spectral region.

The X-ray powder diagrams of the samples investigated are presented in Fig. 2. Contrary to the diagrams of the amorphous dextran powder (A), the curves for dextran samples B, C, and especially D and E indicate the existence of a somewhat higher degree of crystallization. There is some similarity with that reported for crystalline dextran [5]. In fact, the various levels of the crystallization of dextran are expected because dextran is a conformationally labile polymer with very close free conformation energy levels [6]. Thus, the existence of both the "naturally" formed and "induced" insoluble crystalline dextran particles indirectly confirms the mechanism of particle formation and explains the insolubility of the particles.

#### Experimental

##### 1. Materials

The amorphous dextran (m.wt. = 40000) powder (sample A) from Zdravljie (Leskovac, Yugoslavia) was used. The insoluble particles (sample B) were isolated by membrane filtration ( $0.9\text{ }\mu\text{m}$ ) from the sterile glass-bottled solution (10%) prepared from the same amorphous dextran and dried by lyophilization. The induced insoluble particles (sample C) were prepared by treating the glass-bottled dextran solution at  $130\text{ }^{\circ}\text{C}$  for 30 min, according to the mechanism reported elsewhere [3]. The sample D was obtained by heating the amorphous dextran powder at  $130\text{ }^{\circ}\text{C}$  for 30 min. Sample E was, similarly, prepared by evaporation of the 10% dextran solution at  $130\text{ }^{\circ}\text{C}$  followed by heating at the same temperature for 30 min.

##### 2. Measurements

The IR spectra were recorded on an IR spectrophotometer Perkin Elmer, model 580, using the KBr technique. The X-ray powder diagrams were obtained on a Jeol diffractometer using  $\text{CuK}_{\alpha}$  radiation ( $\lambda = 154.178\text{ pm}$ ).

**Acknowledgement:** This study was supported by the Found of Science of Serbia and partly by the Ministry for Science of Macedonia. Special thanks are due to Mr. S. Djordjević from Zdravljie, Leskovac, for supplying the dextran powder and solution.

#### References

- 1 Veljković, V. B.; Lazić, M. L.; Cakić, M. D.: Pharmazie 44, 305 (1989)
- 2 Nakajima, N.; Iwao, Y.; Kuoka, T.; Suzuki, S.; Aizawa, M.: Yagukaku Zasshi 95, 749 (1975)
- 3 Veljković, V. B.; Lazić, M. L.; Cakić, M. D.: Pharmazie 43, 840 (1988)
- 4 Guizard, C.; Chanzy, H.; Sarko, A.: Macromol. 17, 100 (1984)
- 5 Skokova, I. F.; Rodionova, M. I.; Lapshina, G. I.; Homikov, K. P.; Virmik, A. D.; Rogovin, Z. A.; Kozlov, P. V.: Visokomol. Soed. 17, 387 (1975)
- 6 Avsenev, N. N.; Zhbankov, R. G.: SU 973, 545.

Received January 4, 1992

Dr. M. D. Cakić  
University of Niš  
Durmitorska 19  
16000 Leskovac  
  
Dr. G. I. Jovanovski  
Cyril and methodius University  
Skopje  
Yugoslavia

Pharmazie 47 (1992), 1

Martin-Luther-Universität Halle-Wittenberg, Fachbereich Pharmazie, Inst für Pharmazeutische Chemie<sup>1</sup>, und L.A.B. Neu-Ulm, Gesellschaft für pharmakologische Untersuchungen mbH & Co<sup>2</sup>

Di(acyloxy)dialkyl- und Di(acyloxy)diphenylsilane — neue artige Vesikelbildner

Teil 4<sup>3</sup>: Einschluß von Insulin in Siosomen

UTE KUNATH<sup>1</sup>, Z. B. SALAMA<sup>2</sup>, H. RICHTER<sup>1</sup> und P. NUHN<sup>1</sup>

Liposomal verkapselftes Insulin ist schon von zahlreiche Forschungsgruppen untersucht worden [1–7], jedoch gelang es bisher noch nicht, Insulin als vesikuläre Arzneiform zu Anwendung zu bringen.

Nachfolgend wird über den Einschluß von Insulin in Vesikel aus Di(acyloxy)dialkyl- und Di(acyloxy)diphenylsilanen, vor uns erstmals eingesetzte Strukturbildner, berichtet. Die Herstellung der Siosomen erfolgte nach einer speziellen Injektionsmethode, die sich bereits bei anderen Einschlußuntersuchungen bewährt hat [8]. Zur Bestimmung des Insulins diente ein Radioimmunoassay (RIA).

Die Siosomenpräparation erfolgte stets unter konstanten Bedingungen: Ethanolphase: 0,01 mol/l Diacyloxsilan; wäßrige Phase: 3 ml Insulinlösung 0,01 mol/l; Rührgeschwindigkeit:  $2000 \pm 200\text{ U/min}$ ; Temperatur:  $50\text{ }^{\circ}\text{C} \pm 0,1\text{ K}$ . Der Überschuß an nichteingeschlossenem Arzneistoff wurde durch Dialyse an einer Nephrophan<sup>®</sup>-Membran abgetrennt. 1 ml der verdünnten Siosomendispersion (1:8) wurde für mindestens 1 h unter ständiger Aufrechterhaltung des Konzentrationsgefälles dialysiert. Als Dialyseflüssigkeit kam z. B. isotonische Natriumchloridlösung zum Einsatz, andere Lösungen (Kaliumchlorid-, Phosphat-, Phosphat-Albumin-, Krebs-Ringer-Puffer; alle unter Berücksichtigung der Isotonie) wurden ebenfalls in die Untersuchungen einbezogen, wobei die ermittelten Einschlußraten keine wesentlichen Veränderungen zeigten. Die dialysierte Siosomensuspension wurde quantitativ von der Membran gespült und mit Puffer auf 25,0 ml verdünnt. 200 µl wurden zur Bestimmung mittels RIA verwendet [9]. Eine hohe Verdünnung ist wegen der sehr geringen Nachweisgrenze für Insulin (0,1 ng/ml) möglich und erforderlich. Es wurden mindestens 10 identische Versuchsreihen aufgenommen (wegen der relativ hohen Streuung z. T. mehr als 50 Versuchsreihen). Eine Zerstörung der Siosomen ist im Falle des Insulins nicht notwendig, da bereits bei der Aufbereitung der Proben für den RIA die Vesikel wegen der drastisch geänderten osmotischen Verhältnisse (durch Tracerzugabe von 5:1) zerstört werden. Mit Ethanol behandelte Liposomen ergaben deutlich niedrigere Resultate, was auf eine teilweise Denaturierung des Insulins schließen läßt.

Tabelle

Acylketten	Einschlußkapazität	
	[%]	s [%]
Di(acyloxy)dimethylsilane		
decanoxyloxy	63,53	5,97
tetradecanoxyloxy	62,74	8,87
octadecanoxyloxy	79,51	6,29
Di(acyloxy)diphenylsilane		
decanoxyloxy	69,67	8,65
tetradecanoxyloxy	66,60	7,74
octadecanoxyloxy	74,10	10,30
Di(acyloxy)diethylsilane		
decanoxyloxy	67,53	8,52
tetradecanoxyloxy	66,80	4,85
octadecanoxyloxy	54,15	11,80